Journal of King Saud University – Engineering Sciences (2018) 30, 368–376

King Saud University

Journal of King Saud University – Engineering Sciences

www.ksu.edu.sa
www.sciencedirect.com

ORIGINAL ARTICLES

Surface integrity of wire EDMed aluminum alloy: A comprehensive experimental investigation

Pujari Srinivasa Rao [a,*], **Koona Ramji** [b], **Beela Satyanarayana** [c]

[a] *Department of Mechanical Engineering, GITAM University, Visakhapatnam, India*
[b] *Department of Mechanical Engineering, Andhra University, Visakhapatnam, India*
[c] *Department of Mechanical Engineering, Veltech Dr. RR & Dr. SR Technical University, Chennai, India*

Received 16 May 2016; accepted 8 December 2016
Available online 19 December 2016

KEYWORDS

Wire EDM;
Aluminum alloy;
Surface integrity

Abstract A comprehensive experimental investigation in surface integrity is characterized by measurement of residual stresses, altered composition of the surface, surface roughness, white layer thickness, heat affected zone, surface morphology, hardness and corrosion resistance tests. The available literature on surface integrity studies was confined to a few of the above aspects and these studies were mostly concentrated on machining of variety of steels, titanium, inconel and nickel based alloys. In this paper aluminum 2014 T6 alloy has been selected for comprehensive study on surface integrity. The parameter settings influenced the residual stresses and a wide range of values were obtained varying from 8.2 to 405.6 MPa. The effect of parameter settings was also evident on the thickness of white layer and surface morphology. No surface cracks were observed at all machining conditions. The diffusion of elements from wire to surface resulted in the formation of various intermetallic compounds like AlCu and $AlCu_3$ which in turn affected the mechanical and chemical properties of the surface. The elastic properties of intermetallics and galvanic coupling created between the aluminum matrix and intermetallics greatly affected the hardness and corrosion resistance respectively.

1. Introduction

Wire electrical discharge machining (EDM) is an important unconventional machining process. Earlier, the EDM processes were mainly intended for machining of hard metals, but in today's manufacturing sector, they are used for machining of all types of conductive materials due to its ability to machine precise, complex, and irregular shapes of the surfaces (Baraskar et al., 2013; Saedon et al., 2014). But the selection of proper machining condition is essential for obtaining the good surface integrity as it has great impact on parts function.

In view of that many researchers attempted the surface integrity studies on the wire EDMed surface, in which Li et al. (2014) worked on Inconel 718 and evaluated the surface integrity aspects by considering the surface roughness, surface alloying and hardness characteristics. Goswami and Kumar

* Corresponding author. Fax: +91 891 279 0399.
E-mail address: pujari.vizag@gmail.com (P. Srinivasa Rao).
Peer review under responsibility of King Saud University.

ELSEVIER Production and hosting by Elsevier

http://dx.doi.org/10.1016/j.jksues.2016.12.001
1018-3639

(2014) investigated surface integrity aspects in machining of Nimonic alloy 80 A. Material removal rate (MRR) and wire wear ratio were considered as the machining outputs. Anish kumar et al. (2014) presented an experimental investigation on pure titanium and they mainly focused on micro-structural analysis. Li et al. (2013) presented the characteristics of surface integrity versus discharge energy in wire EDM of Inconel 718. Liu et al. (2014) studied surface integrity of shape memory alloy (Nitinol) and explored the machining effects on white layer and hardness. Klocke et al. (2016) investigated the effect of different heat treatments on surface integrity. Two different micro-structural states of the tempering steel 42CrMo4 (AISI4140 steel) were compared based on material removal rate, surface roughness, and recast layer thickness. Navas et al. (2008) performed the surface integrity studies on AISI O1 tool steel components machined by grinding, hard turning and wire EDM. Patel et al. (2009) machined the ceramic composite materials and observed the strength degradation of components due to electric discharge machining. Boujelbene et al. (2009) studied the influence of two types of steels on surface integrity by measuring white layer thickness, MRR, electrode wear rate and micro hardness. The past literature reveals that only a few responses were considered for investigation of surface integrity.

Surface integrity is described by topological, mechanical, metallurgical and chemical conditions of the surface region (Mohammadi et al., 2008). It is characterized by measurement of residual stresses, altered composition of the surface, surface roughness, white layer thickness, heat affected zone, surface morphology, hardness and corrosion resistance tests. In the past literature all the above aspects of surface integrity were not performed on the same specimens, so it is difficult to describe the surface integrity exactly. Moreover, machine tool tables often do not provide the information related to effects of machining condition on properties of machined surface. A comprehensive experimental investigation on surface integrity would be a solution for the above.

As EDM is a thermo electric process, the components machined by this process are influenced by thermal properties of the material especially thermal conductivity and melting point (Khan, 2008). Most of the past literature in EDM processes on surface integrity was limited to machining of Inconel 718, Ti_6Al_4V, various types of steels like AISI H13 tool steel, AISI 304 stainless steel, EN8 medium carbon steel etc. The thermal conductivity and melting point of the above materials were in the range of 6.7–28.6 W/mK and 1336–1660 °C respectively, indicating low thermal conductivity and high melting point. In order to completely study the effect of wire EDM parameters on various materials it was suggested to select a material having properties different from the above, i.e., high thermal conductivity and low melting point. The materials like aluminum alloys possess the above properties and the components made from aluminum alloys are in high demand in aerospace, satellite and defense applications. The latest five-axis machining centers and multi-axis turning centers can produce various shapes of aluminum components with tight tolerances, whereas, wire EDM and sinker EDM machines were generally used for production of complex shapes of aluminum components with extremely tight tolerances in a single setup. Since there was no contact with the workpiece in EDM it produces very fine shapes that were not possible with traditional machining. Hence this process was used for machining of a wide variety of products, such as hydraulic and injection mold components, aerospace structural components, extrusion dies and form tools. With today's high speed wire EDM machines high quality parts can be produced economically (Klocke et al., 2013), but for longevity of the machined components they should possess good surface integrity. The existing literature in WEDM on aluminum alloys was mostly restricted to measuring of a few responses (Selvakumar et al., 2014; Arooj et al., 2014; Ravindranadh et al., 2015) like surface roughness, material removal rate, white layer thickness etc; so there was a dearth of information for finding the effect of wire EDM parameters on surface integrity. The primarily utilized aluminum alloy in aerospace and defense applications is 2024-T4 and for applications where higher strength is required the following alloys 2014-T6, 7075-T6, 7079-T6 and 7178-T6 were commonly used. Aluminum 2014 T6 was used for making wing tension members, shear webs and ribs in aerospace applications.

Here, aluminum 2014 T6 having thermal conductivity of 154 W/mK and melting point 638 °C was selected to find the influence of process parameters on surface integrity.

2. Experimental strategy

Earlier, the authors of this paper had conducted experiments on wire EDM by considering the three parameters as given in Table 1 and investigated the effect of wire EDM conditions on generation of residual stresses in machining of aluminum 2014 T6 alloy and published the same as given in Ref. Rao et al. (2016). In design of experiments the selection of a particular orthogonal array (OA) depends on number of control factors that are of interest, number of levels for each factor, number of runs that can be performed and impact of other conditions such as cost and time. The number of parameters considered in residual stress measurements was 3 with 2 levels each. So, the total number of experimental conditions obtained was 8 ($2^3 = 8$). Hence, L8 orthogonal array was selected to conduct experiments for all 8 possible combinations. The experimental strategy used was full factorial design of high resolution, which facilitates evaluation of main effects (TON, IP, SV), 2-way (TON*IP, IP*SV, SV*TON) and 3-way (TON*IP*SV) interaction effects on residual stresses. Macroscopic residual stresses were measured in aluminum phase and the observed residual stresses are given in Table 2. The further experiments in surface integrity viz., chemical analysis, phase analysis, white layer, surface morphology, hardness and corrosion resistance tests were performed only on identified cases of residual stresses as described in the following Section 2.1.

2.1. Identification of cases

It is difficult to perform all the experiments in surface integrity at all the machining conditions of residual stresses. So, in order

Table 1 Control factors and their levels.

Control factors	Level 1	Level 2	Units
Pulse on time (TON)	105	110	μs
Peak current (IP)	10	12	Ampere
Spark gap voltage (SV)	8	22	Volts

Table 2 The obtained residual stress values in machining of aluminum 2014-T6 (Rao et al., 2016).

Trial No.	Residual stresses (MPa)				
	TON	IP	SV	Replicate 1	Replicate 2
1	105	10	8	67.5	90.6
2	105	10	22	22.1	8.2
3	105	12	8	299.2	309.0
4	105	12	22	269.5	245.8
5	110	10	8	236.4	232.3
6	110	10	22	218.9	229.8
7	110	12	8	405.6	382.0
8	110	12	22	328.2	317.1

to save cost and time three machining conditions were selected from Table 2 for further experiments in surface integrity. In Table 2 it was observed that the highest residual stresses were obtained at the following machining condition of TON = 110 μs, IP = 12 A and SV = 8 V which was referred as case-1 (Trial 7 in Table 2). Similarly the least values of residuals stresses were obtained at the following machining condition TON = 105 μs, IP = 10 A and SV = 22 V which was referred as case-2 (Trial 2 in Table 2). The influence of TON and IP in discharge energy and in turn on generation of residual stresses as in case-1 & 2 is explained here. The basic principle in EDM process is the conversion of electrical energy into heat energy. To control the heat energy one has to control the electrical energy applied across the electrode and workpiece through the electrical parameters like TON and IP (Gaikwad and Jatti, 2018). The energy content of a single spark discharge can be expressed as a product of TON × IP. So the single pulse discharge energy increases with increasing TON and IP values. Investigations on the residual stresses of EDMed components show an increase of their magnitude with increasing pulse energy (Ekmekci, 2007). From the above discussion it is clear that the parameters TON and IP are known for their dominant control or greatest effect in generation of residual stresses (Lee et al., 2011; Younis et al., 2015). Besides TON and IP, SV had also shown significant effects on residual stresses (Rao et al., 2016). Hence, in order to study the effect of SV in the remaining experiments of surface integrity another machining condition at TON = 105 μs, IP = 10 A and SV = 8 V was considered, which was referred as case-3 (Trial 1 in Table 2). The reason for considering case-3 is to facilitate the comparisons between case-1 & 3 (which have the same spark gap voltage i.e. SV = 8 V) and case-2 & 3 (which have the same TON and IP) to find the effect of spark energy and spark gap voltage. In the above three cases cutting speed values were recorded and it is found to be ~3.24, ~0.83 and ~1.37 mm/min in case-1, 2 and 3 respectively.

2.2. Experimental setup

All the machining operations were conducted on Ultra Cut 843/f2 CNC wire EDM. The de-ionized water was used as dielectric fluid and the electrode was zinc coated brass wire. Residual stress measurements were made in the direction of feed using PANalytical X-Pert Pro materials research diffraction (MRD) system. The intermetallic phases which were developed during machining were also identified by the same system. The material used here was aluminum 2014 T6 which is solution heat treated and artificially aged alloy and the as received material was a plate of 150 mm diameter and 10 mm thick. The chemical composition of as received material is confirmed by performing Energy Dispersive X-ray Spectroscopy (EDS) analysis using JEOL JSM-6610LV scanning electron microscope (SEM) and is given in Table 3. At various parameter settings the material was cut into 15 × 20 mm size for performing surface integrity studies. The EDS analysis was also performed on the specimens after undergoing the wire EDM process to find its chemical composition. The white layer measurements were also made using the same equipment, but in a transversal cross section of machined surface. The morphological characterization was done using SEM and stylus type profilometer, Talysurf 10. The cutoff length used for surface roughness measurements was 0.8 mm and an average of five readings was recorded. The SEM photographs were taken with and without applying etchant to observe the possible formation of surface cracks. The composition of etchant used in this investigation was distilled water 92 ml, nitric acid 6 ml, hydrofluoric acid 2 ml and the samples were immersed in this bath for a period of 15 s. Micro-hardness test was conducted on Vickers digital micro hardness tester, DHV-1000, with a load of 2.94 N (300 g) as surface properties are of interest here hence micro hardness measurements are appropriate. The specimens were prepared using smetco polimet-1 for polishing and grinding for a while, not removing the surface layer greater than 2 μm. On each specimen an average of five trials were conducted. The cutting speed values which were displayed on the monitor of the machine tool in mm/min were used for finding the influence of wire EDM parameters on various responses in surface integrity. Pitting corrosion resistance was used to characterize the chemical properties of machined surface in this investigation. A saturated calomel electrode (SCE) and carbon electrodes were used as reference and auxiliary electrodes respectively, and a software based PAR electrochemical system of GILL AC was used to measure

Table 3 Chemical composition of as received aluminum 2014 T6 alloy.

Elements in percentage of weight			
Copper (Cu)	4.70	Titanium (Ti)	0.025
Silicon (Si)	0.74	Chromium (Cr)	0.009
Manganese (Mn)	0.61	Lead (Pb)	0.005
Magnesium (Mg)	0.452	Tin (Sn)	0.005
Iron (Fe)	0.195	Nickel (Ni)	0.003
Zinc (Zn)	0.030	Lithium (Li)	< 0.001
Aluminum (Al)	93.23		

potential. The experiments were conducted in aerated 3.5% NaCl solution with pH adjusted to 10 by adding potassium hydroxide. The potential scan was carried out at 0.166 mV/s with an initial potential of −0.25 V (OC) SCE to final pitting potential and the exposure area for these experiments was 1 cm^2.

3. Results and discussion

3.1. Chemical analysis

The zinc coated copper wire typically alloyed in the range of 63–65% copper and 35–37% zinc was used for machining. The high temperatures generated during machining leads to the diffusion of elements from wire to work surface and changed the composition of the surface. The copper and zinc wt% of the aluminum 2014 T6 alloy before undergone wire EDM process was 4.7 and 0.03 respectively as given in Table 3. The copper and zinc wt% of the samples machined at case-1, 2 and 3 is given in Table 4. An increase in copper and zinc wt% was observed for all the above three cases when compared to as received material which manifests the diffusion of these elements from tool to workpiece. The varied diffusion of these elements may be affected by spark energies which in turn on parameter settings and their levels. With the diffusion of copper, its availability for solid solution with aluminum was increased and led to generation of intermetallic phases of AlCu and $AlCu_3$ as discussed in the following section. The migration of elements from electrode to workpiece was in line with the past literature (Newton et al., 2009).

3.2. Phase analysis

The material under investigation was a 2XXX series type of aluminum–copper (Al–Cu) alloy and therefore different intermetallic compounds of Al–Cu was observed on the machined surface. The X-ray diffraction patterns were depicted for the cases with 1 s per step and varying range from lower side of 10° to a maximum of 120° with a step size of 0.050. The XRD pattern shown in Fig. 1 for case-1 with 2θ angle varying from 85° to 115° shows the $AlCu_3$ (β-phase) at a 2θ angle of approximately 94.5°. Figs. 2 and 3 present the XRD patterns between 40° to 120° and 10° to 120° for case-2 and case-3 respectively. In both the cases Al, AlCu (η-phase) phases were observed at a peak of 52.53° in case-2 and for case-3 the observed peaks are at an angle of 40.62° and 52.55°.

The formation of above intermetallics depends on the formation energies attained in kJ/mol per atom and the availability of copper (Cu) concentration. Phase analysis of Al–Cu alloys in various applications allowed us to identify the following solid solution phases (intermetallic compounds) from the direction of aluminum as Al, AlCu, Al_2Cu, $AlCu_3$, $AlCu_4$, Al_2Cu_3 and Al_4Cu_9 (Trykov et al., 2008). The formation energy of AlCu was less when compared to $AlCu_3$, indicating a relatively weak chemical interaction between Al–Cu (Pismenskaya et al., 2000). Availability of Cu in the bulk material is constant at all the machining conditions, but the diffusion of Cu from tool electrode to workpiece depends on the spark energies and temperatures generated during machining. So, the formation of $AlCu_3$ in case-1, itself indicates the generation of high spark energies and higher Cu availability. In case-2, the formation of AlCu intermetallic indicates lower spark energies as this phase forms at low formation energies, whereas in case-3, the intermetallic obtained was same as in case-2, indicating that the increased spark energies due to lower levels of SV may not be sufficient to form a new phase in the series of Al–Cu intermetallic compounds. The analysis shows that, the interaction effect of SV with TON and IP is most significant, whereas SV as an individual parameter had shown no effect in the formation of new phases.

3.3. White layer thickness (WLT)

The sparks produced during wire EDM process locally melts the material surface and a portion of this molten metal is then ejected and flushed away. The remaining material rapidly re-solidifies to form a surface layer known as the recast layer. This recast layer is referred as white layer since it is difficult to etch and its appearance under optical microscope is white. Beneath the recast layer, a heat affected zone (HAZ) is formed due to rapid heating and quenching cycles during wire EDM. The white layer and HAZ can contain an altered microstructure, tensile stresses, microcracks, impurities, and other undesirable features which can lead to premature part failure when put to service (Newton et al., 2009). Hence the thermal damage caused by EDM has great concern since it will deteriorate surface integrity and functionality of the EDMed components (Guo et al., 2013; Liu et al., 2014). The white layer thickness obtained in case-1, 2 and 3 were ∼50 μm, ∼12 μm and ∼28 μm as shown in Figs. 4–6 respectively.

The WLT values obtained for the above three cases were higher because of the thermal properties of aluminum alloy, which is not desirable. As the portion of the material which experiences thermal effects was more hence more amounts of material were melted, so the dielectric was unable to clear away the material debris, resulting in formation of higher recast layers in this investigation. The higher cutting speed values were indicated by higher spark energies and resulted in thicker

Table 4 Elemental composition of the surface machined at various conditions.

Element	Series	Case-1 Weight%	Case-2 Weight%	Case-3 Weight%
Mg	K	0.39	0.43	0.41
Al	K	82.82	90.39	88.33
Si	K	0.71	0.74	0.74
Cu	L	11.08	6.26	7.65
Zn	L	5.0	2.18	2.87
		100	100	100

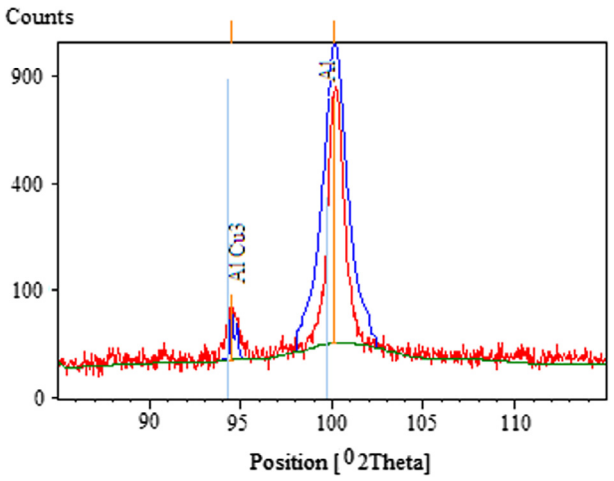

Fig. 1 Plot of XRD pattern for case-1 machining condition.

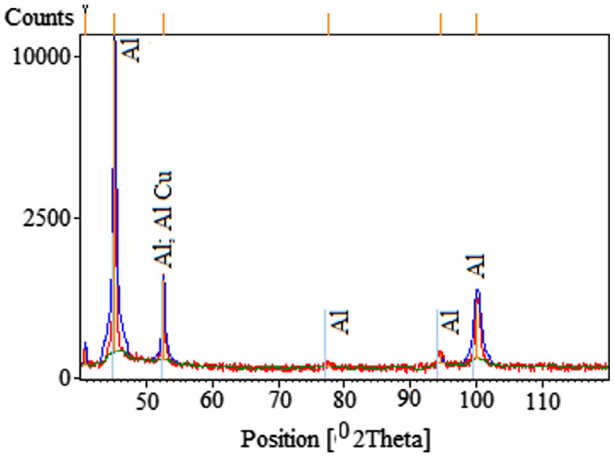

Fig. 2 Plot of XRD pattern for case-2 machining condition.

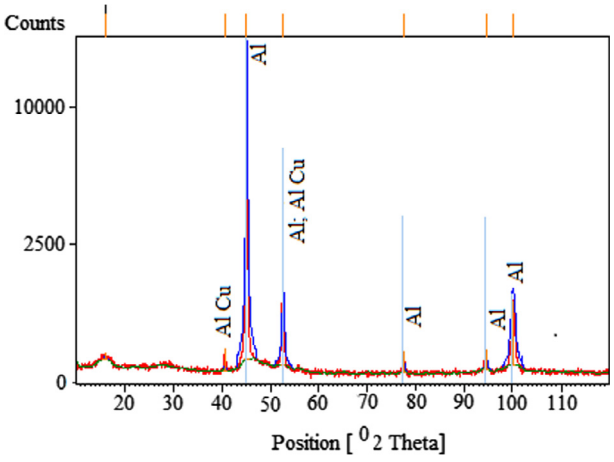

Fig. 3 Plot of XRD pattern for case-3 machining condition.

recast layers as in case-1. At higher values of TON and IP the white layer thickness was observed high as in literature (Dhobe et al., 2013). The effect of SV was estimated by comparing case-3 with case-1 & 2, and a change in WLT of ~22 μm and ~16 μm respectively was observed. From the above results it was found that the parameter SV had considerably influenced the thickness of the white layer. In all the cases heat affected zone (HAZ) was clearly evident. The WLT values in the present investigation were observed high but with the sacrifice of MRR the WLT values can be obtained as low as 3–5 μm for aluminum alloy (Rao et al., 2014).

3.4. Surface morphology

Surface morphology is characterized by surface roughness, ridge-rich surfaces, micro voids and cracks (Guu, 2005). The roughness value of 3.70 μm in case-1, 1.61 μm in case-2 and 2.01 μm in case-3 was measured. The main reason for higher roughness value at case-1 condition is the combined effect of all the parameters. At higher values of TON and IP the discharge energies were high and hence higher roughness was produced. In addition, at lower value of SV the current can take a path of least resistance and a high current arc is seen which damages the workpiece surface resulting in higher roughness. The converse to the above is also true, i.e., lower values of TON and IP gives lower discharge energies and the higher value of SV means that gap is enough for ionization to occur and low current will flow, resulting in lower roughness at case-2 condition. Intermediate value was obtained at case-3 condition.

The obtained SEM photographs as shown in Figs. 7–9 depict a rippled surface, number of cavities and overlapping craters, demonstrate a wire EDM surface, as reported by others (Yan et al., 2005). The slightly wider machined pocks in case-1, micro voids and narrow pocks in case-2, rippled surface in case-3 indicate the variation of discharge energies due to varied parameter settings. The ridge rich surface was formed due to melting and expelling of molten metal during machining and the escape of entrapped gases causes the formation of micro voids.

Surface cracks were not observed at all the cases in this investigation. The formation of surface cracks was attributed to the differentials of high contraction stresses exceeding the material's ultimate tensile strength (Tai and Lu, 2009) but the maximum residual stress value of 405.6 MPa obtained in this investigation is less than the ultimate tensile strength (483 MPa) of aluminum 2014 T6 alloy. As this material is

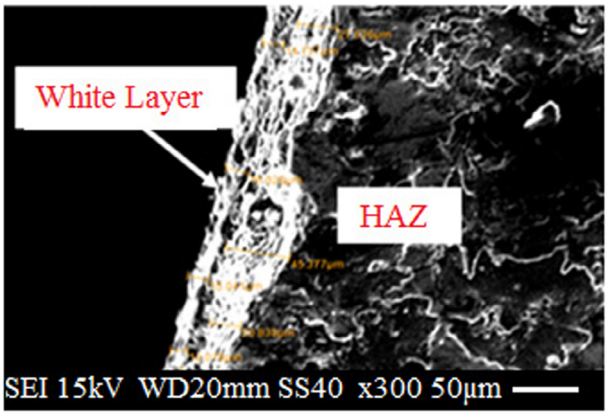

Fig. 4 SEM photograph showing white layer and HAZ at case-1 condition.

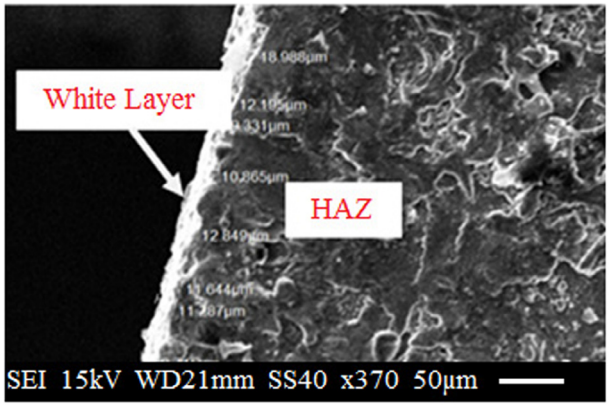

Fig. 5 SEM photograph showing white layer and HAZ at case-2 condition.

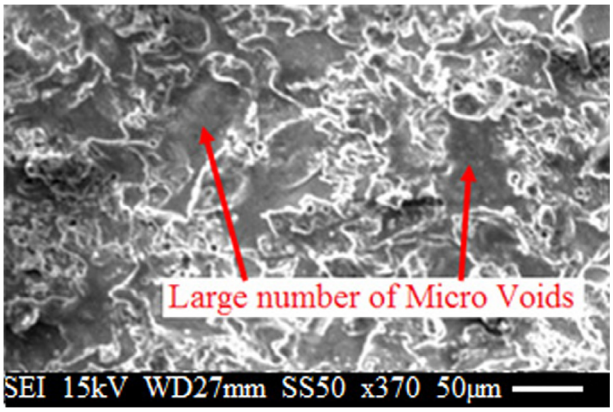

Fig. 8 Microstructure of the wire EDMed surface at case-2 condition.

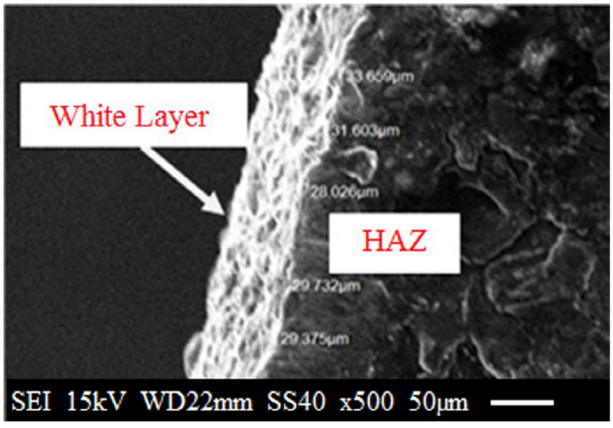

Fig. 6 SEM photograph showing white layer and HAZ at case-3 condition.

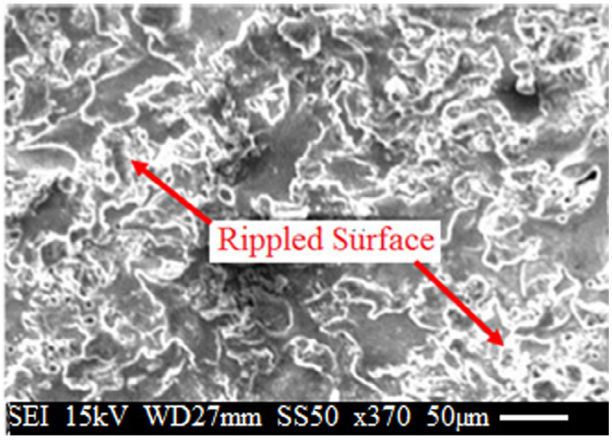

Fig. 9 Microstructure of the wire EDMed surface at case-3 condition.

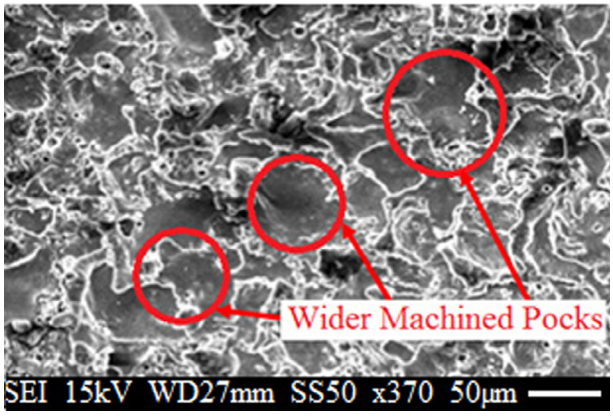

Fig. 7 Microstructure of the wire EDMed surface at case-1 condition.

highly thermally conductive (154 W/m-K), more volume of the material is thermally damaged, but the induced thermal gradients between white layer and bulk material may be not sufficient to generate the cracks. Formation of surface cracks relieves the stress levels on the surface and leads to a shift of peak tensile residual stress to various depth profiles (Kruth and Bleys, 2008). Absence of surface cracks in this investigation indicates that the observed residual stresses on the surface can be considered as a maximum value for that component. This is the reason for not conducting residual stress measurements at various depth profiles. Even though surface cracks were not observed in all the cases, but wider machined pocks, a large number of micro voids and higher roughness values were not advisable for better surface integrity.

3.5. Micro hardness measurement

A marginal increment in hardness was observed on the EDMed surface when compared to as received material. The hardness and standard deviation values for the as received material and the three cases considered are given in Table 5. The reason for the increase in hardness may be due to increased copper content in Al–Cu alloys; which was due to diffusion of Cu from wire to machined surface. In addition, the formation of intermetallic phases may have an effect, since intermetallic phases are harder than their constituent elements (Boukhris et al., 2009).

Increased copper diffusion might increase the hardness but in contrast to that the values were in the decreasing order of

case-2, case-3 and case-1. The AlCu intermetallic possesses higher shear modulus (G) and lower bulk modulus (K) when compared to $AlCu_3$ phase. A low and high value of G/K ratio is associated with ductility and brittleness respectively (Zhou et al., 2009). Hence, higher values of G/K ratio indicate the brittle nature of AlCu when compared to $AlCu_3$. This increased brittleness may have increased the hardness in case-2. The generated residual stresses in wire EDM may be another reason for varied hardness values as it is proved that the residual stresses have an effect on the mechanical properties (Buchheita and Tandon, 2007). A decrease in hardness with increased tensile residual stresses as obtained in this investigation is in-line with the previous literature (Chen et al., 2006). The $AlCu_3$ intermetallic phase was much more anisotropic than other intermetallics (Zhou et al., 2009) results in being directionally dependence of its properties which is not advisable, so its formation must be precluded.

3.6. Pitting corrosion

Wire EDMed surface produces inferior corrosion resistance when compared to surfaces machined by conventional methods (Ntasi et al., 2010). So there is a need to find the effect of wire EDM parameters on corrosion resistance and much research was also not observed in the past literature. Figs. 10 and 11 show the plot of potential versus current density, indicating pitting corrosion behavior of aluminum 2014 T6 alloy before and after undergoing the wire EDM process respectively.

The polarization curve obtained for various cases shows the spontaneous passive material known as protective passive film present on the metal surface at open circuit potential or corrosion potential (E_{corr}). During upward scanning breakdown occurs and a stable pit starts growing at the pitting potential (EP), where the current increases sharply from the passive current level. The materials which exhibit higher values of the EP are generally considered as more resistant to pitting corrosion.

In the present investigation, a substantial improvement in corrosion resistance was observed in all the cases when compared to as received material and the values are given in Table 6. There were many possible reasons for improved and varied pitting corrosion resistance, in which observed intermetallic particles, alloy composition, microstructure, surface condition and residual stresses on the wire EDMed surface can be considered to have a significant effect. Pits in aluminum alloys are typically associated with formation of intermetallic phases in the common Al–Cu intermetallics (Kowal et al., 1996). The phases which are electrochemically nobler than the matrix play the role of cathodes while the matrix undergoes anodic dissolution (Smialowska, 1999) and acts as preferred sites for pitting corrosion through galvanic coupling. Though phase analysis was not performed on as received material, but the E_{corr} value of −727.27 mV manifests the presence of common intermetallic Al_2Cu (θ phase) on aluminum alloy (Muller and Galvele, 1977), which leads to localized corrosion (Chen et al., 1996), such as pitting corrosion, this may be a reason for obtaining lowest corrosion resistance.

The reasons for highest pitting potential observed in case-2 can be explained with the help of magnitudes of measured corrosion potentials for common Al–Cu intermetallics as presented by Mol et al. (2000). The corrosion potentials of

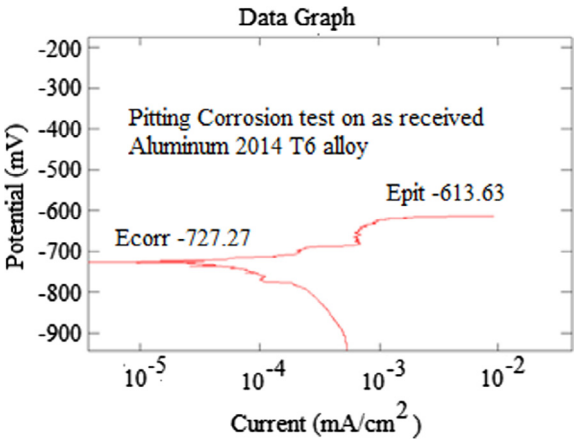

Fig. 10 Polarization curve for as received aluminum 2014 T6 alloy.

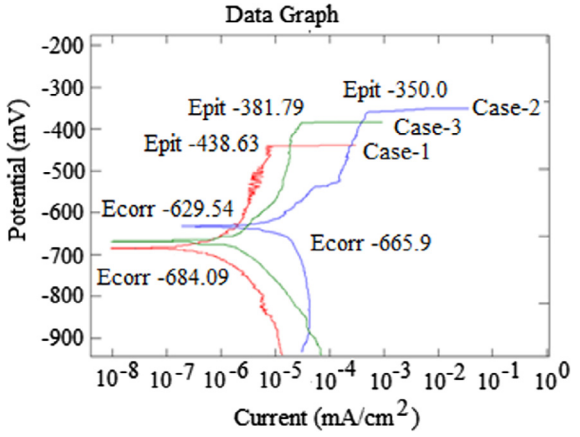

Fig. 11 Polarization curves for surfaces machined at case-1, 2 and 3 conditions.

Table 5 Micro hardness values of aluminum 2014 T6 alloy before and after undergone wire EDM process.

Trial No	Hardness of as received material	Case-1	Case-2	Case-3
1	156.4	157.4	161.4	158.2
2	154.9	153.9	158.8	162.9
3	155.7	166.1	166.5	161.5
4	156.1	156.9	162.2	159.2
5	155.3	155.5	163.7	163.6
Average (HV)	155.68	158.0	162.52	161.08
Standard deviation	0.601664	4.74952	2.84727	2.32744

AlCu and $AlCu_3$ phases were approximately −490 mV and −260 mV respectively (De Wit, 2001) and these values were relatively high when compared to surrounding matrix material with a value of −727.27 mV (Theoretical E_{corr} value of Al 2014 T6 is ~780 mV (Davis, 2000)). So, the above values indicate the cathodic nature of AlCu and $AlCu_3$ with respect to the matrix of aluminum alloy and the difference in potential was

Table 6 Corrosion values of aluminum 2014 T6 alloy before and after undergone wire EDM process.

Trial No	Aluminum 2014 T6 alloy before machining	Case-1	Case-2	Case-3
E_{corr} (mV)	−727.27	−648.09	−629.54	−665.90
Ep (mV)	−613.63	−438.63	−350.00	−381.79

in the range of 235–290 mV and 465–520 mV respectively. Therefore, $AlCu_3$ intermetallic was more cathodic than AlCu intermetallic with respect to aluminum matrix. This high difference in corrosion potential gives the stronger galvanic coupling between aluminum matrix and $AlCu_3$ when compared to AlCu intermetallic. So, the localized attack was expected to be more severe on the components having $AlCu_3$ intermetallic than AlCu, this may be a reason for obtaining better corrosion resistance in case-2 & case-3 when compared to case-1. Surface roughness also had an effect on the corrosion resistance. In general, samples prepared with a rough surface finish are more susceptible to pitting and exhibits a lower pitting potentials (Laycock and Newman, 1997). Its effect on pitting corrosion is related to the stabilization criteria because rougher surfaces have more occluded sites, which can sustain the conditions required for active dissolution at lower current densities and thus produces lower potentials. The highest surface roughness obtained in case-1 may also be a reason for obtaining lowest corrosion resistance, whereas in case-2 & 3 the variations in roughness values may vary the corrosion resistance even though the observed intermetallic phases were same. The highest residual stresses observed in case-1 was another reason for obtaining the lowest pitting potential, as higher tensile residual stresses adversely affect the pitting corrosion resistance (Boven et al., 2007). The negligible residual stress observed in case-2 may have acted favorably in obtaining higher corrosion resistance. So in order to have better resistance to corrosion hence better surface integrity the surface has to be machined at low spark energies.

4. Conclusions

The aim of the present investigation was fulfilled by considering all aspects in surface integrity studies on aluminum 2014 T6 alloy.

- At lower values of pulse on time and peak current and higher value of spark gap voltage low or negligible residual stress value of 8.2 MPa was observed.
- Migration of Cu and Zn elements from the wire to surface and formation energies attained during machining influenced the formation of intermetallic phases of AlCu and $AlCu_3$.
- At low discharge energy conditions better morphological characteristics were obtained in terms of lower roughness value and narrow machined pocks. Surface cracks were not observed at all the machining conditions.
- A wide range of WLT values were observed ranging from 12 μm to 50 μm. The obtained values for aluminum alloy were slightly high when compared to other metals. But with the sacrifice of MRR the WLT values can be obtained as low as 3–5 μm.
- The elastic properties of intermetallics in terms of G/K ratio and residual stresses influenced the hardness value of wire EDMed aluminum alloy. The observed hardness values were slightly high when compared to as received material. The $AlCu_3$ intermetallic was anisotropic in nature and its formation must either be controlled or prevented.
- The $AlCu_3$ intermetallic was much more cathodic when compared to AlCu with respect to Aluminum. The galvanic coupling created between the Al and AlCu was the main reason for obtaining higher corrosion resistance value. In addition, a low surface roughness of 1.61 μm and lower residual stress value of 8.2 MPa were also the reasons for obtained good corrosion resistance.

From the results of the investigation a relationship can be established between cutting speed and various responses in surface integrity. With the increase in cutting speed the higher values of residual stresses, white layer, surface roughness, and poor mechanical and chemical properties were observed which is not advisable. So for better surface integrity the parameters should be set at lower levels of pulse on time and peak current in combination with higher values of spark gap voltage.

Acknowledgement

The authors would like to thank Sri. R.V.S. Subrahmanyam, Scientist-G, Naval Science and Technological Laboratory, Visakhapatnam, India, for extending his support during experiments.

References

Arooj, S., Shah, M., Sadiq, S., Jaffery, S.H.I., Khushnood, S., 2014. Effect of current in the EDM machining of aluminum 6061 T6 and its effect on the surface morphology. Arab. J. Sci. Eng. 39, 4187–4199.

Baraskar, S.S., Banwait, S.S., Laroiya, S.C., 2013. Multiobjective optimization of electrical discharge machining process using a hybrid method. Mater. Manuf. Process. 28, 348–354.

Boujelbene, M., Bayraktar, E., Tebni, W., Salem, S.B., 2009. Influence of machining parameters on the surface integrity in electrical discharge machining. Arch. Mater. Sci. Eng. 37, 10–116.

Boukhris, N., Lallouche, S., Debilia, M.Y., Draissia, M., 2009. Microhardness variation and related microstructure in Al–Cu alloys prepared by HF induction melting and RF sputtering. Eur. Phys. J. Appl. Phys. 45, 30501–30508.

Boven, G.V., Chen, W., Rogge, R., 2007. The role of residual stress in neutral pH stress corrosion cracking of pipeline steels. Part I: pitting and cracking occurrence. Acta Mater. 55, 29–42.

Buchheita, T.E., Tandon, R., 2007. Measuring residual stress in glasses and ceramics using instrumented indentation. J. Mater. Res. 22, 2875–2887.

Chen, G.S., Gao, M., Wei, R.P., 1996. Microconstituent-induced pitting corrosion in aluminum alloy 2024-T3. Corrosion 52, 8–15.

Chen, X., Yan, J., Karlsson, A.M., 2006. On the determination of residual stresses and mechanical properties by indentation. Mater. Sci. Eng. A 16, 139–149.
Davis, J.R., 2000. Corrosion of Aluminum and Aluminum Alloys. ASM International, United States of America.
De Wit, J.H.W., 2001. New knowledge on localized corrosion obtained from local measuring techniques. Electrochim. Acta 46, 3641–3650.
Dhobe, M.M., Chopde, I.K., Gogte, C.L., 2013. Investigations on surface characteristics of heat treated tool steel after wire electro-discharge machining. Mater. Manuf. Process. 28, 1143–1146.
Ekmekci, B., 2007. Residual stresses and white layer in electric discharge machining (EDM). Appl. Surf. Sci. 253, 9234–9240.
Gaikwad, V., Jatti, V.S., 2018. Optimization of material removal rate during electrical discharge machining of cryo-treated NiTi alloys using Taguchi's method. J. King Saud Univ. Eng. Sci. 30 (3), 266–272.
Goswami, A., Kumar, J., 2014. Investigation of surface integrity, material removal rate and wire wear ratio for WEDM of Nimonic 80 A alloy using GRA and Taguchi method. Eng. Sci. Technol. 17, 173–184.
Guo, Y., Klink, A., Fu, C., Snyder, J., 2013. Machinability and surface integrity of nitinol shape memory alloy. CIRP Ann. 62, 83–86.
Guu, Y.H., 2005. AFM surface imaging of AISI D2 tool steel machined by the EDM process. Appl. Surf. Sci. 242, 245–250.
Khan, A.A., 2008. Electrode wear and material removal rate during EDM of aluminum and mild steel using copper and brass electrodes. J. Mater. Process. Technol. 39, 482–487.
Klocke, F., Zeis, M., Klink, A., Veselovac, D., 2013. Technological and economical comparison of roughing strategies via milling, sinking-EDM, wire-EDM and ECM for titanium- and nickel-based blisks. CIRP J. Manuf. Sci. Technol. 6, 198–203.
Klocke, F., Schneider, S., Ehle, L., Meyer, H., Hensgen, L., Klink, A., 2016. Investigations on surface integrity of heat treated 42CrMo4 (AISI 4140) processed by sinking EDM. Proc. CIRP 42, 580–585.
Kowal, K., Deluccia, J., Josefowicz, J.Y., Laird, C., Farrington, G.C., 1996. In-situ atomic-force microscopy observations of the corrosion behavior of aluminum-copper alloys. J. Electrochem. Soc. 143, 2471–2481.
Kruth, J.P., Bleys, P., 2008. Measuring residual stresses caused by wire EDM of tool steel. Int. J. Elec. Mach. 5, 23–28.
Kumar, A., Kumar, V., Kumar, J., 2014. Surface integrity and material transfer investigation of pure titanium for rough cut surface after wire electro discharge machining. Proc. Inst. Mech. Eng. Part B 228 (8), 880–901.
Laycock, N.J., Newman, R.C., 1997. Localised dissolution kinetics, salt films and pitting potentials. Corros. Sci. 39, 1771–1790.
Lee, H.T., Tai, T.Y., Liu, C., Hsu, F.C., Hsu, J.M., 2011. Effect of material physical properties on residual stress measurement by EDM hole-drilling method. J. Eng. Mater. Technol. 133, 0210141–0210148.
Li, L., Guo, Y.B., Wei, X.T., Li, Y.W., 2013. Surface integrity characteristics in wire-EDM of inconel 718 at different discharge energy. Procedia CIRP 6, 220–225.
Li, L., Wei, X.T., Li, Z.Y., 2014. Surface integrity evolution and machining efficiency analysis of W-EDM of nickel-based alloy. Appl. Surf. Sci. 313, 138–143.
Liu, J.F., Li, L., Guo, Y.B., 2014. Surface integrity evolution from main cut mode to finish trim cut mode in W-EDM of shape memory alloy. Appl. Surf. Sci. 308, 253–260.
Mohammadi, A., Tehrani, A.F., Emanian, E., Karimi, D., 2008. A new approach to surface roughness and roundness improvement in wire electrical discharge turning based on statistical analysis. Int. J. Adv. Manuf. Technol. 39, 64–73.
Mol, J.M.C., Hinton, B.R.W., Weijde, D.H.V.D., Dewit, J.H.W., Zwaag, S.V.D., 2000. A filiform corrosion and potentiodynamic polarisation study of some aluminium alloys. J. Mater. Sci. 35, 1629–1639.
Muller, I.L., Galvele, J.R., 1977. Pitting potential of high purity binary aluminium alloys-II and Al–Zn alloys. Corros. Sci. 17, 995–1007.
Navas, V.G., Ferreres, I., Maranon, J.A., Rosales, C.G., Sevillano, G. J., 2008. Electro discharge machining (EDM) versus hard turning and grinding-comparison of residual stresses and surface integrity generated in AISI 01 tool steel. J. Mater. Process. Technol. 195, 186–194.
Newton, T.R., Melkote, S.N., Watkins, T.R., Trejo, R.M., Reister, L., 2009. Investigation of the effect of process parameters on the formation and characteristics of recast layer in wire-EDM of Inconel 718. Mater. Sci. Eng. 513, 208–215.
Ntasi, A., Mueller, W.D., Eliades, G., Zinelis, S., 2010. The effect of electro discharge machining (EDM) on the corrosion resistance of dental alloys. Dent. Mater. 26, 237–245.
Patel, K.M., Pulak, M., Pandey, P., Rao, P.V., 2009. Surface integrity and removal mechanisms associated with the EDM of Al2O3 ceramic composite. Int. J. Refract. Met. Hard Mater. 27, 892–899.
Pismenskaya, E.B., Rogachev, A.S., Kovalev, D.Y., Ponomarev, V.I., 2000. The mechanism of formation of copper aluminide in the thermal explosion mode. Russ. Chem. Bull. 49, 1954–1959.
Rao, P.S., Ramji, K., Satyanarayana, B., 2014. Experimental investigation and optimization of wire EDM parameters for surface roughness, MRR and white layer in machining of aluminium alloy. Procedia Mater. Sci. 5, 2197–2206.
Rao, P.S., Ramji, K., Satyanarayana, B., 2016. Effect of wire EDM conditions on generation of residual stresses in machining of aluminum 2014 T6 alloy. Alexandria Eng. J. 55, 1077–1084.
Ravindranadh, B., Madhu, V., Gogia, A.K., 2015. Multi response optimization of wire-EDM process parameters of ballistic grade aluminium alloy. Eng. Sci. Technol. 18, 720–726.
Saedon, J.B., Jaafar, N., Jaafar, R., Saad, N.H., Kasim, M.S., 2014. Modeling and multi-response optimization on WEDM Ti6Al4V. Appl. Mech. Mater. 510, 123–129.
Selvakumar, G., Sornalatha, G., Sarkar, S., Mitra, S., 2014. Experimental investigation and multi-objective optimization of wire electrical discharge machining (WEDM) of 5083 aluminum alloy. Trans. Nonferrous Met. Soc. China 24, 373–379.
Smialowska, Z.S., 1999. Pitting corrosion of aluminium. Corros. Sci. 41, 1743–1767.
Tai, T.Y., Lu, S.J., 2009. Improving fatigue life of electro-discharge-machined SKD11 tool steel via the suppression of surface cracks. Int. J. Fatigue 31, 433–438.
Trykov, Y.P., Slautin, O.V., Arisova, V.N., Shmorgun, V.G., Pomomareva, I.A., 2008. Effect of technological factors on the diffusion kinetics in the copper-aluminum composite. Russ. J. Non-Ferrous Metals 49, 42–48.
Yan, B.H., Tsai, H.C., Huang, F.Y., Lee, L.C., 2005. Examination of wire electrical discharge machining of Al2O3p/6061Al composites. Int. J. Mach. Tools Manuf 45, 251–259.
Younis, M.A., Abbas, M.S., Gouda, M.A., Mahmoud, F.H., Abd Allah, S.A., 2015. Effect of electrode material on electrical discharge machining of tool steel surface. Ain Shams Eng. J. 6, 977–986.
Zhou, W., Lijuan, L., Baoling, L., Song, Q., Ping, W., 2009. Structural, elastic, and electronic properties of Al–Cu intermetallics from first-principles calculations. J. Electron. Mater. 38, 356–364.